DOI:10.1021/jf100356a

JOURNAL OF AGRICULTURAL AND FOOD CHEMISTRY
ARTICLE

Feruloyl Dioleoylglycerol Antioxidant Capacity in Phospholipid Vesicles

Joseph A. Laszlo,*,† Kervin O. Evans,† Karl E. Vermillion,‡ and Michael Appell§

†Renewable Product Technology, USDA-Agricultural Research Service, National Center for Agricultural Utilization Research, 1815 N. University Street, Peoria, Illinois 61604, ‡Functional Foods Research, USDA-Agricultural Research Service, National Center for Agricultural Utilization Research, 1815 N. University Street, Peoria, Illinois 61604, and §Bacterial Foodborne Pathogens and Mycology, USDA-Agricultural Research Service, National Center for Agricultural Utilization Research, 1815 N. University Street, Peoria, Illinois 61604

Ferulic acid and its esters are known to be effective antioxidants. Feruloyl dioleoylglycerol was assessed for its ability to serve as an antioxidant in model membrane phospholipid vesicles. The molecule was incorporated into single-lamellar vesicles of 1,2-dioleoyl-*sn*-glycero-3-phosphocholine at 1 and 5 mol fractions. Employing a lipid peroxidation inhibition assay, feruloyl dioleoylglycerol was demonstrated to express an oxidation protection ratio relative to Trolox of 0.94 and 0.74 at the 1% and 5% incorporation levels, respectively. The impact of feruloyl dioleoylglycerol incorporation on vesicle integrity was examined by determining calcein—cobalt complex leakage rates. Vesicle leakage was not influenced at 22 or 37 °C with 5% feruloyl dioleoylglycerol incorporation in comparison to that of vesicles lacking feruloyl dioleoylglycerol. Resonance energy transfer analysis showed that the closest approach distance between feruloyl dioleoylglycerol and 1,2-dioleoyl-*sn*-glycero-3-phospho-L-serine-*N*-(7-nitro-2-1,3-benzoxadiazol-4-yl) was approximately 31 Å, which indicated that feruloyl dioleoylglycerol was thoroughly distributed throughout the bilayer plane. Conformational analysis determined that feruloyl dioleoylglycerol has a splayed conformation in which its feruloyl moiety is not closely contacted by its oleoyl groups. Feruloyl dioleoylglycerol integrates into the bilayer with its feruloyl moiety oriented close to the hydrophilic/lipophilic interface and its oleoyl groups extended deeply in the membrane. These findings indicate that feruloyl dioleoylglycerol expresses antioxidant activity by intercepting aqueous-phase free radicals as they penetrate the bilayer.

KEYWORDS: Ferulic acid; triglyceride; antioxidant; membrane bilayer; resonance energy transfer (RET); density functional theory; molecular modeling; nuclear Overhouser effect spectroscopy (NOESY)

INTRODUCTION

The cinnamates ferulic acid (3-(3′-methoxy-4′-hydroxyphenyl)-propenoic acid) and caffeic acid (3-(3′,4′-dihydroxyphenyl)-propenoic acid) are common and plentiful dietary components (*1*, *2*). Derived from plant sources, ferulic and caffeic acids come as both free acids and various esters thereof. Their esters are found predominately as architectural components of the hemicellulose and lignin fractions of the plant cell wall, as well as in suberin and cutin waxy surfaces of leaves and other plant parts. Feruloyl esters of ω-hydroxyalkanoic acids and long-chain alkan-1-ols have been isolated from potato periderm (*3*, *4*). A caffeoyl-ω-hydroxyfatty acyl glycerol was isolated from cotton (*5*). Feruloyl glycerols have been identified (*3*, *6*). Ferulic acid is found esterified to phytosterols in grain products such as corn and rice bran oils (*7*). Caffeic acid is widely found as conjugates of quinic acid and related hydroxy acids (*1*). Just as this multitude of cinnamate conjugates has broad utility in plants, animals too may have many avenues to exploit these molecules.

Because of their anticipated low toxicity, cinnamate derivatives have been closely examined for their medicinal value (*8*). Alkyl esters of ferulic and caffeic acid are able to perform as anti-inflammatories and cancerogenesis suppressors. Murakami and co-workers (*9*, *10*) found that 2-methyl-1-butyl ferulate attenuated the inflammatory events of inducible nitric oxide synthase/cyclooxygenase-2 expression and superoxide anion generation. This molecule also suppressed phorbol ester-induced Epstein−Barr virus activation and papilloma development in mouse skin. Long-chain alkyl esters of caffeic acid inhibit nitric oxide production in murine macrophage cells, suggesting an anti-inflammatory activity (*11*). Ferulate and caffeic alkyl esters demonstrate anti-tumor proliferation activity with colon breast, lung, and gastric human cell lines, as well as inhibition of COX-1 and COX-2 enzymes (*12*). All these activities are attributable to the cellular

*Corresponding author. Tel: 309-681-6322. Fax: 309-681-6686. E-mail: Joe.Laszlo@ars.usda.gov.

 Published on Web 04/15/2010

incorporation efficacies of the lipophilic cinnamates. However, significant cytotoxicity occurs with long-chain alkyl esters of ferulic or caffeic acids (*11*, *13*). It thus may be valuable to look for cinnamate derivatives displaying lower cytotoxic potential while retaining the indicated beneficial attributes.

Lipid peroxidation products of polyunsaturated fatty acids play a major role in genotoxicity of the cell (*14*). Free radical-initiated lipid peroxidation causes the loss of membrane structure and so too gives rise to toxic products such as 4-hydroxyalkenals and other aldehydes that in principle can move from the site of origin and produce effects in distant proteins and nucleic acids. Such distal molecular structures are protected by antioxidant quenching of free-radical propagation events in membranes. The physiological influences evinced by lipophilic cinnamates may in part be a result of their substantial antioxidant capacity. Lipophilic cinnamate esters of vegetable oils are readily produced by enzymatic transesterification (*16*). In vitro tests of feruloyl dioleoylglycerol (FDOG) demonstrated that these compounds have significant antioxidant capacity (*17*). However, there is much to learn about the physiological performance of such cinnamate esters.

A detailed understanding of the biological mechanisms by which lipophilic cinnamate esters elicit their various effects is lacking. Single-lamellar phospholipid vesicles can serve as convenient models for cellular membranes. Demonstration of antioxidant incorporation into such vesicles should be central to having the expected lipid protection effect. Furthermore, minimal loss of vesicle integrity with antioxidant insertion may serve as a measure of low cytotoxicity potential. FDOG was examined in the present work to determine whether it incorporates into phospholipid vesicles with the retention of antioxidant capacity and without membrane integrity disruption. The localization of the feruloyl group within the phospholipid bilayer was investigated to determine its proximity to potential oxidation-sensitive lipid double-bond sites. Conformational analysis was employed to assess FDOG structure and orientation within the bilayer.

MATERIALS AND METHODS

Reagents and Materials. Ethyl ferulate was obtained from Sinova Corp. (Ningbo, China). Triolein, ferulic acid 2,2-diphenyl-1-picrylhydrazyl (DPPH), cobalt(II) chloride hexahydrate, ethylenediaminetetraacetic acid disodium dehydrate (EDTA), 2,2′-azobis(2-amidinopropane) dihydrochloride (AAPH), and Triton X-100 were purchased from Sigma-Aldrich (St. Louis, MO). Novozym 435 was purchased from Novozymes through Brenntag Great Lakes (Chicago, IL). 1,2-Dioleoyl-*sn*-glycero-3-phosphocholine (DOPC), 1, 2-dioleoyl-*sn*-glycero-3-phospho(TEMPO)-choline (TEMPO-PC), 1-palmitoyl-2-stearoyl-(5-DOXYL)-*sn*-glycero-3-phosphocholine (5DOXYL-PC), 1-palmitoyl-2-stearoyl-(12-DOXYL)-*sn*-glycero-3-phosphocholine (12DOXYL-PC), and 1,2-dioleoyl-*sn*-glycero-3-phospho-L-serine-*N*-(7-nitro-2-1,3-benzoxadiazol-4-yl) (ammonium salt) (NBD-PS) were purchased from Avanti Polar Lipids (Alabaster, AL). High purity calcein and 4,4-difluoro-5-(4-phenyl-1,3-butadienyl)-4-bora-3a,4a-diaza-*s*-indacene-3-undecanoic acid (C_{11}-Bodipy 581/591) were purchased from Invitrogen (Carlsbad, CA). Potassium phosphate monobasic, potassium phosphate dibasic, Sephadex G-75 column beads, columns, and sodium chloride were all obtained from Fisher Scientific.

Feruloyl Dioleoylglycerol (FDOG) Preparation. Ethyl ferulate (2.5 g), triolein (10 g), and immobilized *Candida antarctica* lipase B (2.5 g of Novozym 435) were combined and shaken at 60 °C for one week (*15*, *18*). Novozym 435 was removed by filtration (nylon filter). The reaction product was subjected to flash chromatography using a C18 reverse phase column and a 60:40 v/v acetonitrile/acetone solvent, with UV detection at 340 nm. The FDOG containing peak was subjected to further purification by HPLC using a Luna semipreparative phenylhexyl column (250 mm ×10 mm, 10 μm; Phenomenex, Torrance, CA) developed with methanol at a flow rate of 5 mL/min. Details of analytic HPLC and mass spectroscopy procedures have been given previously (*18*). The FDOG product was an oil at room temperature. ^{1}H NMR (d_6-acetone): δ (ppm) 7.65 (1 H, d, =CH-Ar), 7.37 (1 H, s, Ar−H), 7.16 (1 H, d, Ar−H), 6.89 (1 H, d, Ar−H), 6.43 (1 H, d, CH=CH-Ar), 5.36 (m, 2-CH_2CH=CHCH_2), 4.1−4.5 (4 H, m, 2-CH_2O), 3.95 (3 H, s, OCH_3), 2.35 (m, 2-$CH_2CH_2CO_2$), 2.04 (m, 2-$(CH_2CH_2)_2$CH=CH), 1.63 (m, 2-$CH_2CH_2CH_3$), 1.38 (m, 18-$CH_2CH_2CH_2$), 0.90 (m, 2-CH_3). $^{13}C\{^1H\}$ NMR (d_6-acetone): δ (ppm) 172.3 ($CH_2CH_2CO_2$), 166.2 (CH=CHCO_2), 149.4 (Ar), 148.0 (Ar), 145.7 (Ar-CH=), 130.0 (2-CH_2CH=CHCH_2), 126.5 (Ar), 123.3 (Ar), 115.2 (Ar), 114.1(CH=CHCO_2), 110.4 (Ar), 69.2 (CH$(CH_2O-)_2$), 61.9 (CH$(CH_2O-)_2$), 55.6 (CH_3O), 33.7 (2-$CH_2CH_2CO_2$), 31.6 (2-$CH_2CH_2CH_3$), 29.1 (aliphatic), 27.0 (2-CH_2CH=CHCH_2), 24.8 (2-CH_2CH_2CH=CH CH_2CH_2), 22.7 (2-CH_3CH_2-), 13.5 (2-CH_3-). Electrospray ionization mass spectroscopy (ESI-MS): 795.7 $[M - H]^-$ (calcd $C_{49}H_{80}O_8$: 796.6). FDOG molar absorptivity: 1.93×10^4 M^{-1} cm^{-1} at 325 nm in ethanol.

On the basis of ^{1}H NMR and heteronuclear multiple bond correlation (HMBC) analysis, it was determined that of the two potential FDOG regioisomers, 88% was 1(3)-feruloyl-2,3(1)-dioleoyl glycerol and 12% was 2-feruloyl-1,3-dioleoyl glycerol (see Supporting Information).

DPPH Assay. The free radical scavenging capability of FDOG, was determined using the DPPH assay with modifications as described by Choo and Birch (*17*). DPPH spontaneously forms a free radical in solution. FDOG (2.5 mM) was mixed with 0.2 mM DPPH in ethanol. Ferulic acid and ethyl ferulate were also examined for comparison. DPPH radical reduction was followed spectrophotometrically at 517 nm for 30 min at 2-min intervals using a Shimadzu 1240 UV−vis spectrophotometer. The reaction was conducted at room temperature (approximately 23 °C). Triplicate runs of antioxidant at each concentration were performed. The percentage of DPPH radical remaining over time was calculated as the sample absorbance divided by that of a control DPPH sample at the same time, multiplied by 100.

Lipid Preparation and Formation of Unilamellar Phospholipid Vesicles. Lipids and vesicles were prepared in a manner similar to that used by MacDonald and co-workers (*19*) with some modifications. Lipids were prepared from appropriate amounts of DOPC in chloroform and FDOG (at 1- or 5-mol % of total lipids) in ethanol added to clean amber vials and then gently mixed. Chloroform and ethanol were removed by warming and gently blowing argon into the vials for several minutes until a dried lipid film was present. Residual solvent was removed by keeping the dried films under vacuum overnight. The dried lipid films were stored under argon at −20 °C until needed.

To form phospholipid vesicles, the dried lipid films were allowed to equilibrate to ambient temperature, rehydrated in the appropriate buffer, and mixed periodically over an hour. The multilamellar vesicles that formed from the rehydration were then put through five freeze−thaw cycles (using 2-propanol on dry ice and water heated to 60 °C). These vesicles were then extruded 11 times through two, stacked, polycarbonate 100-nm filters in a LiposoFast extruder (Avestin, Inc.; Ottawa, Canada) to form unilamellar vesicles (approximately 125 nm in diameter). Vesicles were covered with argon, protected from light, and stored at 4 °C until used.

Vesicle Leakage (Calcein−Cobalt). Vesicles with and without FDOG were evaluated for membrane integrity using a leakage assay described by Evans (*20*). The column buffer was modified to include 17 mM NaCl for osmotic balance during the separation of the vesicles from the unincorporated calcein−cobalt complex. The leakage assay was designed such that the low fluorescent signal of the entrapped calcein−cobalt complex increased as vesicles leaked their contents, and cobalt was stripped from calcein by external EDTA. Vesicle leakage was monitored spectroscopically on a Fluorolog 3-21 fluorometer. The excitation and emission wavelengths were 490 and 520 nm, respectively, with 2-nm slit widths apiece. Samples were continuously stirred in 1-cm path length quartz cuvettes. Measurements were recorded for 30 min at 5-s intervals. Experiments were conducted in triplicate at 22 and 37 °C using a total lipid concentration of 0.15 mM. Leakage percentage was determined from the intensity of the fluorescent signal, $100 \times (F_t - F_o)/(F_{max} - F_o)$, where F_t was the fluorescent signal over time, F_o was the extrapolated initial signal at time zero, and F_{max} was the fluorescent signal at the end of the experiment after complete rupture by addition of 1% v/v aqueous Triton X-100 solution (20 μL added to 2 mL to make a final concentration of 0.01% v/v Triton X-100). The apparent rate constant k was obtained by fitting to the equation: $F_t = F_{max}(1 - \exp(-kt))$.

Lipid Oxidation Inhibition. Lipid oxidation inhibition by FDOG was measured by the lipid peroxidation inhibition capacity (LPIC) assay, which employs AAPH as a free-radical initiator and the lipidic reporter molecule C_{11}-Bodipy (*21*). DOPC and C_{11}-Bodipy were combined in a vial, dried to a film, and then rehydrated in 20 mM Tris-HCl, pH 7.4, to give a concentration of 5.0 mM DOPC and 4.8 μM C_{11}-Bodipy. FDOG (at 1- or 5-mol % of DOPC) from ethanol was included in the preparation of the DOPC/C_{11}-Bodipy lipid film prior to the formation of vesicles, in those instances where FDOG LPIC was determined. Unilamellar vesicles were prepared from rehydrated lipids as described above. Samples were diluted to a final concentration of 2.5 mM DOPC and 2.4 μM C_{11}-Bodipy and allowed to equilibrate to 37 °C for 15 min prior to measurement. From the time of AAPH addition (40 mM final concentration), fluorescence intensity (excitation at 540 nm, emission at 595 nm) was measured every minute for 180 min. Experiments were conducted in triplicate. The relative fluorescence intensity was calculated by dividing the reading at each minute by the initial fluorescence at the beginning of the experiment (F_t/F_o). Background subtraction was accomplished using vesicles containing only DOPC.

The water-soluble antioxidant Trolox was used for comparison. Trolox was combined with DOPC and C_{11}-Bodipy, dried, and then rehydrated as described above. A Trolox concentration range of 10 to 125 μM (before dilution with AAPH) was employed. The peroxyl radical scavenging capacity of FDOG relative to Trolox (relative antioxidation activity) was calculated using the following equation:

$$= \frac{(AUC_{Sample} - AUC_0)}{(AUC_{Trolox} - AUC_0)} \times \frac{mol_{Trolox}}{mol_{Sample}} \quad (1)$$

where AUC_{Sample} is the area under the fluorescence curve (AUC) for vesicles containing antioxidant (Trolox or FDOG), AUC_{Trolox} is the area under the curve for vesicles containing 50 μM Trolox (thereby arbitrarily assigned a relative antioxidation activity value of 1.0), AUC_0 is the area under the curve for vesicles containing only Bodipy, and mol_{Sample} is the molar concentration of the antioxidant (*22*). The AUC was calculated by three different methods: those described by Cao and co-workers (*23*), Naguib (*24*), and Zhang and co-workers (*21*).

FDOG Bilayer Distribution Using Fluorescent Probe Energy Transfer. The mobility and distribution of FDOG in the bilayer was determined from the resonance energy transfer technique (*25*, *26*). FDOG was treated as the donor and NBD-PS as the acceptor. Vesicles contained 1-mol % FDOG with 0.01-, 0.1-, or 1.0-mol % NBD-PS, or 5-mol % FDOG with 0.05-, 0.5-, or 5.0-mol % NBD-PS. Measurements were conducted in 10 mM potassium phosphate buffer, pH 7.0, at 37 °C. Fluorescence emission spectra were recorded using an excitation wavelength of 330 nm. The excitation and emission slit widths were 5 nm. Spectral scattering and NBD-PS contributions to the emission spectra were taken into account by subtracting the spectra of vesicles containing the appropriate concentration of NBD-PS absent FDOG.

An overlap of the excitation of NBD-PS (acceptor) with the emission spectrum of FDOG (donor) indicated that resonance energy transfer was possible (see Supporting Information, Figure 8). This spectral overlap allowed the determination of the Förster radius (R_o) according to the Förster equation:

$$R_o = 0.211[\kappa^2 n^{-4} Q_D J(\lambda)]^{1/6} \quad (2)$$

where Q_D is the quantum yield of FDOG in the absence of NBD-PS, n is the refractive index of the bilayer, $J(\lambda)$ is the overlap integral between FDOG and NBD-PS, and κ is the orientation factor of the transition dipoles of FDOG and NBD-PS (assumed to be 2/3 for dynamic random averaging for donor−acceptor pair). The distance from the bilayer center for the NBD group was assumed to be 18.8 Å at pH 7.0 (*27*) .

Feruloyl Group Bilayer Location Using Nitroxide-Labeled Lipids. The depth of the feruloyl group of FDOG within the vesicle phospholipid bilayer was determined by parallax analysis at 37 °C (*28*, *29*). Briefly, FDOG fluorescence intensity was reduced by collisional quenching caused by nitroxide-labeled phosphatidylcholine (PC). The nitroxide-labeled lipids used had the nitroxide quencher positioned in the headgroup region (TEMPO-PC), just below the headgroup region (5DOXYL-PC), or farther down the acyl chain (12DOXYL-PC). Conceptually, FDOG should experience the most quenching from the nearest nitroxide group, therefore allowing calculation of the distance between feruloyl group and the bilayer center. Nitroxide-labeled lipids were separately incorporated at 15 mol % into the membrane in conjunction with FDOG at various concentrations. Measurements were conducted in potassium phosphate buffer at pH 7.0. Fluorescence emission spectra were recorded using an excitation wavelength of 330 nm. The excitation and emission slit widths were 5 nm. A background emission was subtracted using DOPC vesicles, with or without nitroxide-labeled lipids as appropriate.

The difference in quenching of FDOG by the nitroxide-labeled lipids indicates a difference in depth penetration by FDOG in the membrane. Accordingly, the quenching differences allow the calculation of the probable location of FDOG in a membrane using the pallalax equation (*29*) as follows:

$$z_{cf} = L_{c1} + [-\ln(F_1/F_2)/\pi C - L_{21}^2]/2L_{21} \quad (3)$$

In the parallax eq 3, z_{cf} is the distance the fluorophores are from the center of the membrane, F_1 is the normalized emission fluorescence intensity (normalized in respect to vesicles with FDOG only) in the presence of the shallow quencher, F_2 is the normalized fluorescence intensity in the presence of the deep quencher, L_{c1} is the distance between the shallow quencher and the center of the bilayer, C is the concentration of quenchers per area (mole fraction of nitroxide-labeled lipids/area of lipid), and L_{21} is the difference in depth between quenchers. The area of the phosphatidylcholine lipids was taken to be 70.1 Å^2 per molecule (*30*), and the distances from the bilayer center for the nitroxide group were assumed as 19.5 Å for TEMPO-PC, 12.2 Å for 5DOXYL-PC, and 5.9 Å for 12DOXYL-PC (*28*). Preliminary tests found that the best results using the strongest quenching pairs (shallow versus deep quenchers) were TEMPO-PC/DOPC versus 5DOXYL-PC/DOPC for vesicles containing 1.0 mol % FDOG and 5DOXYL-PC/DOPC versus 12DOXYL-PC/DOPC for vesicles with 5.0-mol % FDOG.

Conformational Analysis. *NMR Analysis.* ^{1}H nuclear Overhauser effect spectroscopy (NOESY) was conducted on a Bruker Avance 500 spectrometer using a 5-mm BBO probe with Z-gradient and Topspin 1.3 software. The sample was dissolved in $CDCl_3$ and degassed with bubbling argon. Spectra were acquired at 300.0 K. Chemical shifts are reported as parts per million from tetramethylsilane based on the lock solvent. The NOESY spectrum was acquired with a mixing time of 0.5 s using the Bruker pulse program noesyetgp. There were 96 acquisitions per slice, and the total experiment time was approximately 19 h.

Molecular Modeling. Initial structures were built using the AMBER force field as implemented in the HyperChem v7.52 program (Hypercube Inc., Gainsville, Florida). This force field approach was demonstrated to be suitable for the conformational analysis of related lipids (*31*). Quantum chemical calculations were carried out using Parallel Quantum Solutions hardware and software (v3.2) (Parallel Quantum Solutions, Fayetteville, Arkansas). Select conformations were investigated using Becke's three parameter functional with Lang−Yang−Paar functionals (B3LYP) at the 6-311++g(d,p) level. Unless otherwise noted, geometry optimizations were performed with the convergence criteria set at 1×10^{-6} Hartree and a gradient of less than 3×10^{-4} a.u. using the eigenvector following algorithm. The Conductor-like screening model (COSMO) continuum solvation model was employed for implicit solvation (chloroform) (*32*). The additional atomic radius for solvent accessible surfaces was set at 2.48 Å with the electrical permittivity of the dielectric continuum set at 4.90. Results were imaged using Hyperchem v7.52.

RESULTS

DPPH Antioxidant Capacity. The antioxidant activity of a phenolic compound is attributable to its scavenger activity toward several free radicals, such as alkyl, alkoxyl, and peroxyl radicals (R•, RO•, and ROO•, respectively). Such radicals are formed during the oxidation of fats and oils. The rapidity and completeness with which an antioxidant reacts with the stable free radical DPPH• in organic solvent is a common measure of antioxidant capacity. **Figure 1** demonstrates that FDOG had an antioxidant capacity greater than that of ferulic acid or ethyl ferulate on an equivalent molar basis. Triolein does not quench

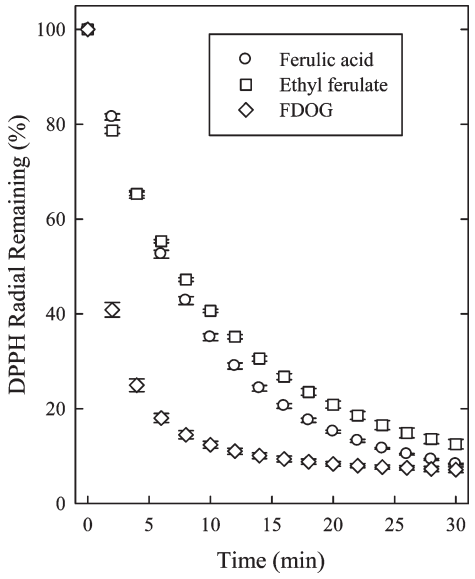

Figure 1. Time course for the reaction of ferulate species with the DPPH free radical. The concentrations were 2.5 mM for FDOG, ferulic acid, or ethyl ferulate. Error bars represent one standard deviation from the mean ($n = 3$).

DPPH• (*17*), indicating that the feruloyl moiety was responsible for the observed scavenging activity. In our hands, FDOG was far more reactive with DPPH• than previously reported (*17*). Using the same solvent (ethanol) and 25 mM FDOG, a 10-fold higher concentration of FDOG than employed herein, Choo and Birch (*17*) observed poor scavenging activity (approximately 35% DPPH• remaining after 30 min). They found 25 mM ferulic acid to be much more capable than FDOG as a DPPH• scavenger (less than 10% DPPH• remaining after 2 min with ferulic acid). The reason for the DPPH activity disparity in FDOG results is unclear.

Lipid Peroxidation Inhibition. The ability of FDOG to express its antioxidant properties under conditions more relevant to an in vivo molecular environment was examined. FDOG was incorporated into unilamellar phosphocholine vesicles and subjected to oxidative conditions using the free-radical initiator AAPH. C_{11}-Bodipy, which fluoresces until oxidized, served as a reporter lipid within the vesicles to follow the progression of the free-radical attack on the membrane. The conventional antioxidant Trolox also was examined to provide a basis for comparison.

Figure 2 (upper panel) shows the time-dependent relative fluorescence of C_{11}-Bodipy in the presence of 40 mM AAPH and varying Trolox concentrations. With no AAPH present, the relative fluorescence of C_{11}-Bodipy remained steady, demonstrating the stability of the probe under these conditions. Upon the addition of AAPH, the relative fluorescence rapidly decreased, as would be expected when no antioxidant protection of C_{11}-Bodipy was provided. With Trolox present, a plateau in the relative fluorescence developed and extended with increased concentration of Trolox, as demonstrated by Zhang and co-workers (*21*). A linear correlation between the net area under the curve (ΔAUC) and Trolox concentration was also evident (**Figure 2**, upper panel, insert).

Figure 2 (lower panel) shows the relative fluorescence of C_{11}-Bodipy in the presence of FDOG at two different concentrations (1 and 5 mol %). FDOG exhibited no plateau phase in the relative fluorescence like that provided by Trolox. However, the decay rate of the C_{11}-Bodipy relative fluorescence with FDOG present was slower than the decay rate without FDOG. The fluorescence

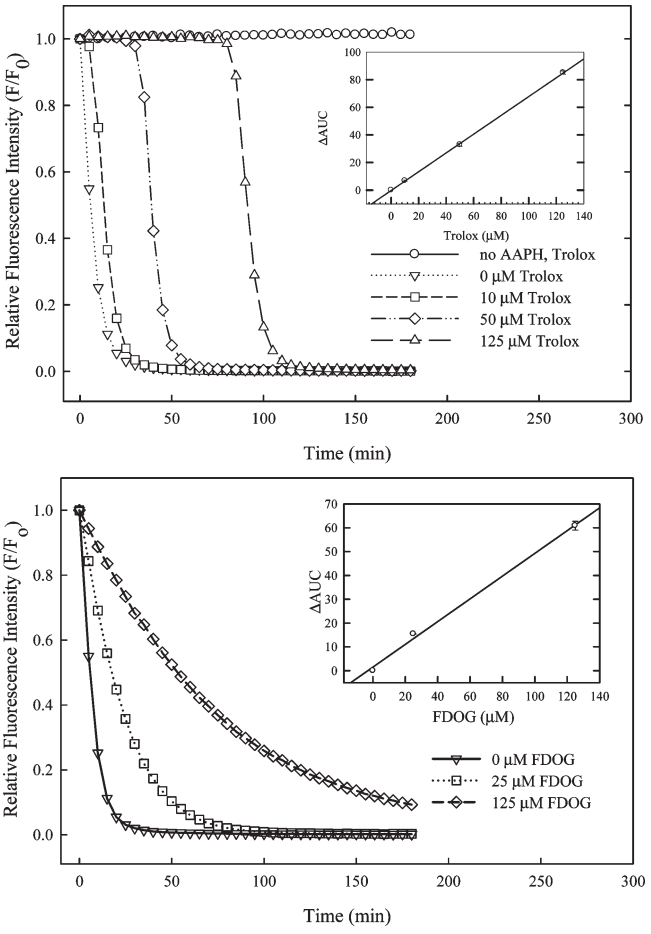

Figure 2. Comparison of lipid peroxidation inhibition capacities of Trolox and FDOG in DOPC vesicles at 37 °C. Upper panel: relative fluorescence changes of C_{11}-Bodipy in the presence of 40 mM AAPH and Trolox at various concentrations. The insert is a plot of the net area under the curve (ΔAUC) versus Trolox concentration. Lower panel: relative fluorescence changes of C_{11}-Bodipy in the presence of 40 mM AAPH and FDOG at various concentrations (0, 1, and 5 mol % of total lipids). The insert is a plot of the ΔAUC versus FDOG concentration.

decay rate also decreased with increased FDOG concentration, and the ΔAUC for FDOG demonstrated a linear correlation with concentration (**Figure 2**, lower panel, insert).

The ratio of antioxidant activity of 1- and 5-mol % FDOG relative to Trolox (eq 1) was determined to be 0.94 and 0.74, respectively (**Table 1**). This lower relative antioxidant activity value and the lack of a plateau region indicated that FDOG, although able to retard oxidation, was not as capable of an antioxidant as Trolox under the conditions of the assay. However, these results confirmed that FDOG retains its antioxidation capacity when incorporated into a model phospholipid bilayer.

Vesicle Leakage. The ability of FDOG to destabilize phospholipid vesicles was determined by monitoring the release of entrapped contents (calcein−cobalt complex). **Figure 3** shows that the leakage of DOPC vesicles at 22 °C proceeded equally with or without FDOG present. Further analysis of the kinetics confirmed that vesicle leakage was not altered by FDOG inclusion in the membrane at this temperature (**Table 2**). At a higher, physiologically significant temperature (37 °C), vesicles exhibited a slightly increased leakage rate, as expected (*33*). Again, FDOG incorporation at 1- and 5-mol % levels did not significantly ($P > 0.05$) alter the leakage rate relative to that of vesicles lacking FDOG (**Table 2**). Small changes in leakage rates are ascribed to

Table 1. Relative Antioxidant Capacity of Trolox and FDOG in the LPIC Assay

		relative antioxidant capacity[a]		
antioxidant	concentration (μM)	AUC method A	AUC method B	AUC method C
Trolox	10	1.03	1.03	1.03
Trolox	50	1.00	1.00	1.00
Trolox	125	1.04	1.04	1.04
FDOG	25	0.94	0.94	0.94
FDOG	125	0.74	0.75	0.74

[a] Relative antioxidant activity calculated according to eq 1. Method A: AUC calculated according to Zhang and co-workers (*21*). Method B: AUC calculated according to Cao and co-workers (*23*). Method C: AUC calculated according to Naguib (*24*).

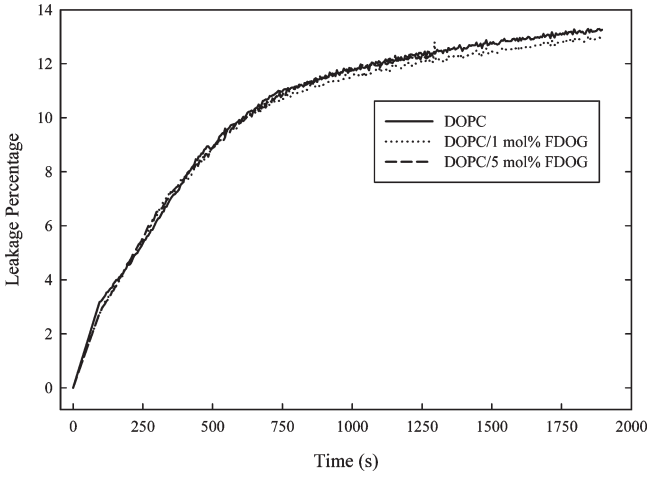

Figure 3. Time dependence of calcein−cobalt leakage from the DOPC vesicle without and with 1- or 5-mol % FDOG at 22 °C. Data displayed represent the mean values of triplicate analyses.

changes in membrane fluidity (*33*). An order of magnitude increase in leakage rates would be expected for small pore formation, and instantaneous leakage would be observed with vesicle disruption (*34*). Therefore, over the temperature range explored FDOG did not induce any substantial disturbance of the phospholipid bilayer fluidity or intactness that could be correlated with changes in the release rate of vesicle-entrapped contents.

Mobility and Distribution in the Membrane. That membrane-incorporated FDOG displays antioxidant capacity and does not adversely modify membrane permeability suggests the molecule is mobile and distributed throughout the membrane plane. To test this hypothesis, the average distance between FDOG and other vesicle phospholipids was determined. The NBD-PS excitation spectrum and FDOG fluorescence emission spectrum were found to overlap (Supporting Information, Figure 8). Therefore, these two molecules made a good resonance energy transfer pair (nonradiative dipole−dipole coupling) that could be used to calculate the Förster distance, i.e., the distance at which the energy transfer efficiency is 50%, between FDOG and NBD-PS. To calculate the Förster distance, a corrected emission spectrum and the quantum yield of FDOG were needed. On the basis of the method described by Peng and co-workers (*35*) and using 9,10-diphenylanthracene as the reference standard (quantum yield of 0.95 (*36*)), the quantum yield of FDOG was determined to be 0.55 in ethanol and 0.08 in DOPC vesicles. The Förster distance for FDOG in DOPC vesicles was therefore calculated to be approximately 29.8 Å.

When the sample was excited at 330 nm, nearly all of the fluorescence at 530 nm was from NBD-PS (Supporting Information, Figure 8). This means that the equation for energy transfer efficiency ($E = 1 - F_{DA}/F_D$, where F_{DA} and F_D are the fluorescence of the donor in the presence and absence of the acceptor, respectively) is valid. Therefore, the energy transfer efficiency was used to calculate the closest approach distance between FDOG and NBD-PS to be approximately 31 Å. This is well within the range of closest approach distances found for other fluorescent lipids (*26*).

Energy transfer can occur between donor−acceptor pairs that are both in the same bilayer plane (leaflet) and the opposing bilayer plane. Therefore, the closest approach distance determined here is an average of energy transfer occurring within the

Table 2. Rates of Calcein−Cobalt Complex Leakage from DOPC Vesicles with or without Incorporated FDOG

temperature (°C)	FDOG (mol %)	leakage rate constant (ms^{-1})
22	0	2.24 ± 0.32
22	1	2.29 ± 0.16
22	5	2.32 ± 0.35
37	0	2.57 ± 0.07
37	1	3.65 ± 0.78
37	5	2.40 ± 0.64

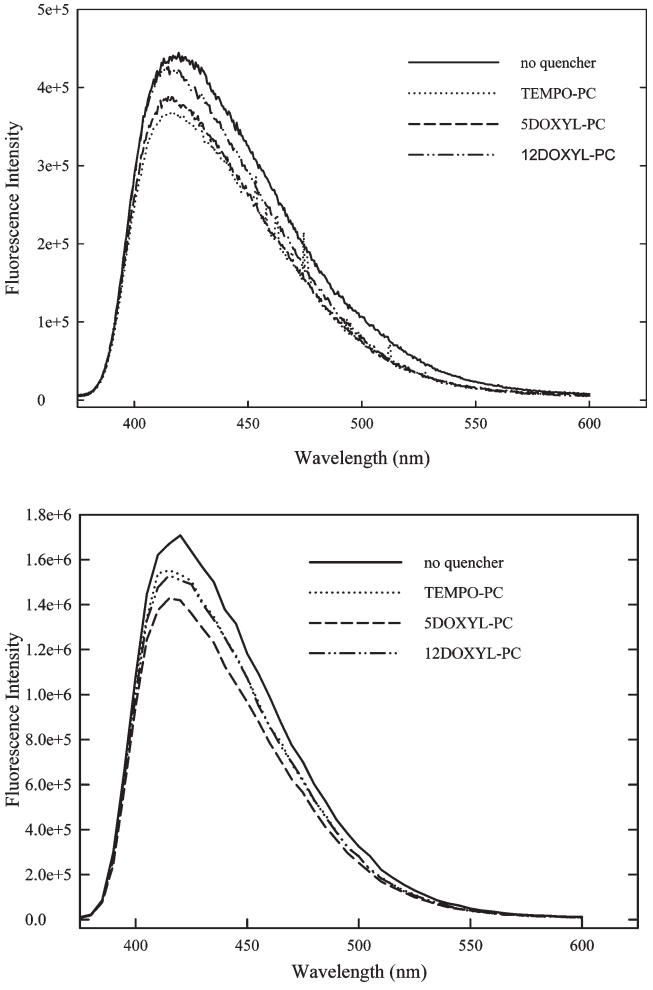

Figure 4. Fluorescence spectra of FDOG at (upper panel) 1 mol % and (lower panel) 5 mol % in phospholipid vesicles with and without quenchers. The composition of the vesicles was DOPC/FDOG (no quencher, 99:1 or 99:5), DOPC/TEMPO-PC/FDOG, DOPC/5DOXY-PC, or 12DOXYL-PC (all at 84:15:1 or 80:15:5).

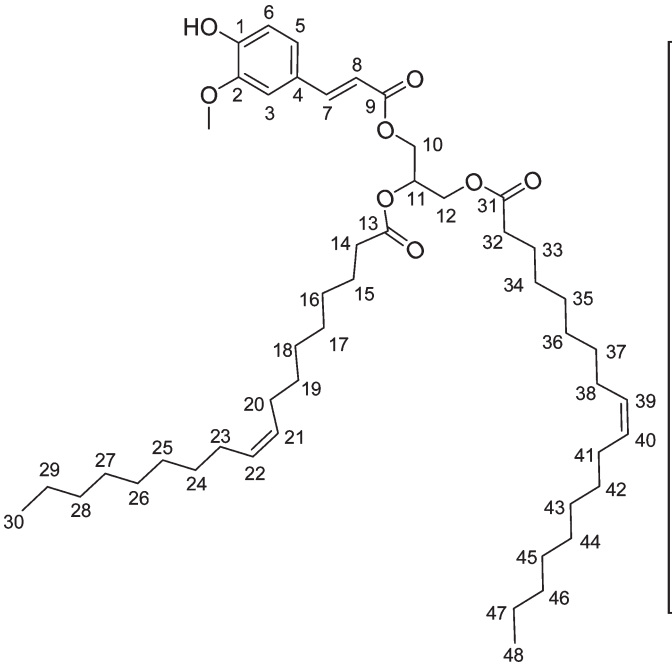

NOE cross-peak assignments

7 ↔ 3, 5
7 ↔ 8
5 ↔ 6
3, 5 ↔ 8
3 ↔ OCH_3
11 ↔ 10, 12
21, 22, 39, 40 ↔ 20, 23, 38, 41
21, 22, 39, 40 ↔ envelope
14, 32 ↔ 15, 33
14, 32 ↔ envelope
20, 23, 38, 41 ↔ envelope
15, 33 ↔ envelope
30, 48 ↔ envelope

Figure 5. NOESY analysis of FDOG intramolecular interactions. The data were collected with FDOG dissolved in $CDCl_3$ using a 500 MHz instrument.

same bilayer plane and between opposite planes. Assuming that energy transfer between FDOG and NBD-PS does occur between pairs within the same bilayer plane and pairs in opposite planes, then the closest approach distance determined here suggests that FDOG and NBD-PS in opposite bilayer planes are able to pass over the top of one another. The interpretation that FDOG and NBD-PS can pass over the top of one another further suggests that FDOG does not have restricted movement within the bilayer. The closest approach distance further excludes the possibility that FDOG formed domains, such as those observed with cholesterol in bilayers. Typical domain sizes are 100 to 2000 Å. It would be expected that if FDOG formed domains the closest approach distance between NBD-PS and FDOG would fall more within the range of typical domain sizes. Therefore, FDOG at 1- and 5-mol % appeared to be mobile and uniformly dispersed throughout the bilayer, not sequestered in isolated domains such as those observed with cholesterol in phospholipid bilayers.

Feruloyl Group Membrane Depth. FDOG incorporated at 1- and 5-mol % in DOPC vesicles had a strong fluorescent signal, as can be observed in **Figure 4**. Fluorescence quenching of FDOG was exhibited by phosphatidylcholine molecules bearing nitroxide groups at various depths within the vesicle membrane. This allowed the distance from the center of the bilayer, z_{cf}, of FDOG's fluorophore, the feruloyl moiety, to be estimated (eq 3). Distances of 16.8 ± 1.4 Å and 15.7 ± 0.9 Å were calculated for 1- and 5-mol % FDOG, respectively. These values are not significantly different ($P = 0.2$); therefore, a mean value of 16.3 ± 1.2 Å was assumed. This distance places the feruloyl moiety within the beginning of the hydrophilic region of the DOPC bilayer just above the hydrophobic layer, but not fully extended into the aqueous media (*30*, *37*).

Conformational Analysis. NOESY analysis of FDOG was conducted to identify the salient intramolecular interactions (**Figure 5**). The NOESY spectrum (Supporting Information, Figure 7) showed the expected interactions of the feruloyl moiety's olefin protons with each other and to the aromatic protons. The methoxy protons interact with an aromatic proton. The glyceryl protons also have the expected cross-talk peaks, as

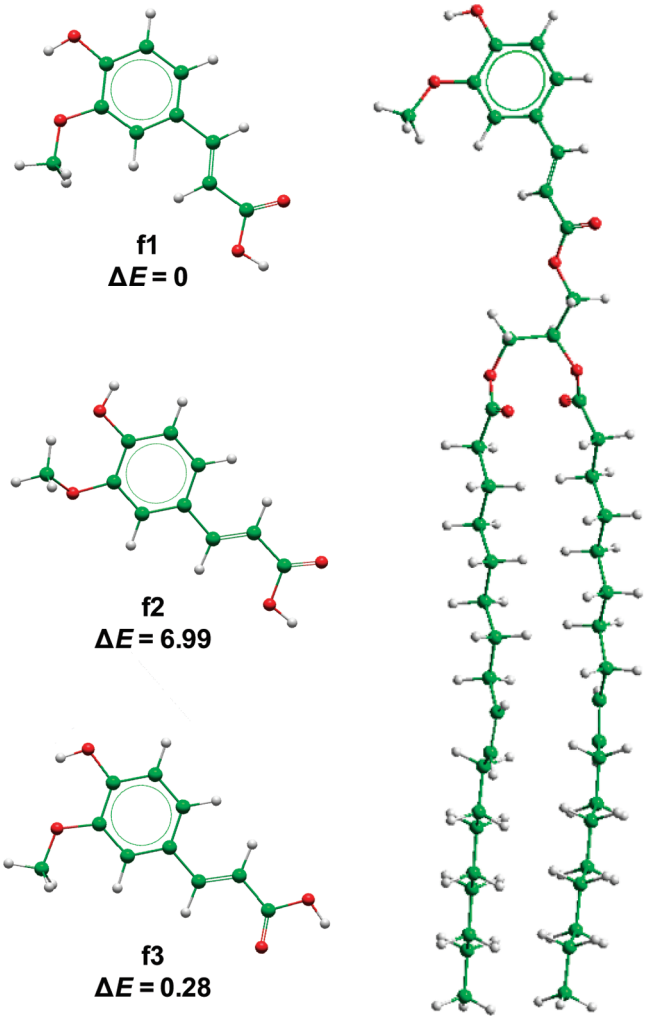

Figure 6. Conformers of FDOG and ferulic acid (**f1**, **f2**, and **f3**). Relative energies are in kcal/mol. Carbon atoms are displayed in green, oxygen atoms in red, and hydrogen atoms in white.

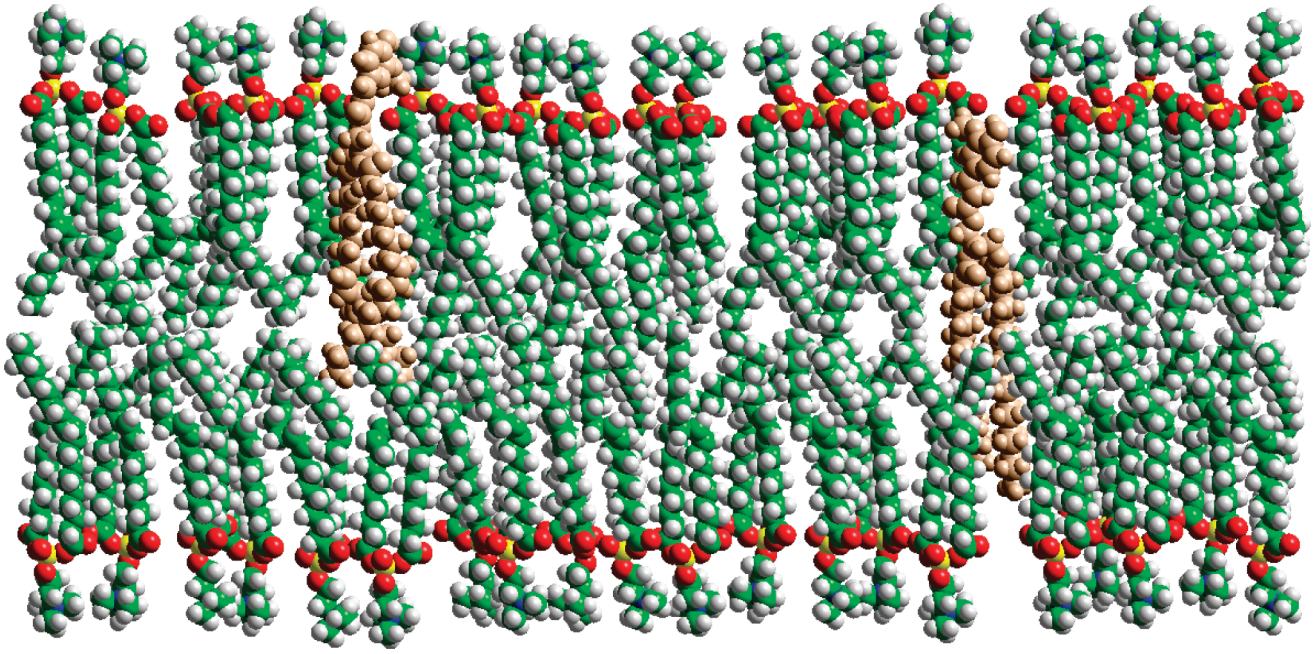

Figure 7. Molecular representation of FDOG embedded in a DOPC bilayer (5-mol % FDOG). FDOG is represented in brown. For DOPC, carbon atoms are displayed in green, oxygen atoms in red, nitrogen atoms in blue, and hydrogen atoms in white. Calculations were carried out using the AMBER force field to position the molecular components. A simple, two-molecule deep representation of the bilayer was extracted to facilitate visualization, which accounts for the apparent void spaces in the image.

do the oleoyl moieties, but there was no indication that the feruloyl group interacts, within the 4.5-Å limit of detection, with either the glyceryl or acyl fatty acid features of the molecule. The lack of intramolecular interactions between the feruloyl moiety and the glycerol backbone or the other acyl chains is in marked contrast to that reported for ferulates esterified directly to straight, long-chain alkyl groups (*31*, *38*). NOESY experiments are relatively insensitive; therefore, there were no discernible cross-peaks associated with the 12% 2-feruloyl-1,3-dioleoylglycerol regioisomer present in the sample.

FDOG is a large lipid with a feruloyl moiety, glycerol linker, and two oleic acid chains (**Figure 5**). Smaller but structurally similar molecules have been investigated using the B3LYP density functional at the 6-31G(d,p) level, including caffeate and gallate esters (*13*,*39*), ferulic acid (*38*,*40*−*42*), and hydroxycinnamic acid derivatives (*43*, *44*). Initial attempts to geometry optimize the complete structures of FDOG were complicated by incomplete convergence, possibly due to shallow minimization wells associated with the oleic chains. To address this issue, geometry optimization first was carried out on the feruloyl moiety. A conformational analysis of ferulic acid was carried out at the B3LYP/6-311++G(d,p) level. A preferred conformation, **f1** (**Figure 6**), compared favorably with the experimental NOESY findings. This structure possesses several signals observable by NOESY experiments, with a distance of 2.38 Å between the hydrogen of the methoxy substituent and the C3−H. The distance between the aromatic C3−H and the C8−H of the olefin is 2.20 Å. The conformation features a favorable 2.09 Å hydrogen bond between the hydrogen of the C1 phenolic hydroxyl and the oxygen of the methoxy substituent. A recent density functional study investigated conformation **f2** of ferulic acid, which lacks this hydrogen bond interaction (*40*); however, this structure was found to be unfavorable, and higher in energy by 6.99 kcal/mol in vacuo over conformation **f1** (5.42 kcal/mol higher in chloroform). The experimental NMR data indicated NOE signals between both the C3−H and C5−H with the C7−H of the olefin. The distance between the C3−H with the C7−H in conformer **f3** is 2.32 Å, and this conformation is within 0.28 kcal/mol of the preferred conformation **f1** ($\Delta E_{Chloroform}$ = 0.13 kcal/mol). These calculations matched the NOESY analysis and suggest that FDOG can adopt two stable orientations of the ferulic acid moiety (**Figure 6**, **f1** and **f3**). The entire FDOG molecule optimized at the PM3 level is shown in **Figure 6**. Again, these calculations matched the NOESY analysis, which found no interaction of the oleic acid groups with the feruloyl moiety.

A model showing the FDOG in a dioleoyl phosphatidylcholine membrane bilayer is given in **Figure 7**. The length of extended FDOG is approximately 33 Å, in contrast to the approximate 27 Å length of dioleoyl phosphatidylcholine. The feruloyl moiety oriented so as to be near the hydrophobic/hydrophilic interface, which is consistent with its placement determined by resonance energy transfer measurements. The oleoyl groups reach deeply into the bilayer and can extend across to the opposing leaflet. Thus the conformational analyses indicated that FDOG exhibits a splayed structure and that the entire, extended FDOG molecule can be embedded within the dioleoyl phosphatidylcholine membrane bilayer.

DISCUSSION

Hydroxycinnamates such as ferulic acid have been the subject of extensive research because of their potential to counteract the destructive action of reactive oxygen species. Antioxidant efficacy reflects both its inherent reactivity (antioxidant capacity) and proximity to those structures requiring protection. Hydroxycinnamic acids and their hydrophilic esters are expected to be useful for guarding against oxidation of aqueous phase cellular components (e.g., proteins and nucleic acids). Lipophilic hydroxycinnamate esters would be expected to perform in membranes. Thus, drawing marginal distinctions between whether a molecule is a better antioxidant in its water-soluble form (e.g., ferulic acid) or in its lipophilic form (e.g., FDOG), on the basis of measures such as the DPPH assay, are of limited physiological significance. To assess antioxidant efficacy for membrane lipids, an antioxidant

must demonstrate (1) a free-radical scavenging capacity (such as by the DPPH method), (2) the ability to partition into membranes at a significant concentration without disrupting the integrity of the membrane, (3) an antioxidant capacity while incorporated into a membrane, and (4) the prevention of ROS initiated destruction of lipids proximal to the membrane-incorporated antioxidant.

FDOG was shown to have a free-radical scavenging capacity (**Figure 1**). This is consistent with the findings of others with lipophilic ferulate esters (*17*, *31*, *45*−*47*) and related phenols (*48*−*50*). A range of ferulate alkyl esters (saturated C_7 to C_{18}, linear, and branched) showed similar DPPH scavenging activity (*31*). This indicates that with saturated alkyl groups the side chain length is not an important influence on antiradical activity under homogeneous conditions such as the DPPH assay. This is true for gallate esters as well (*48*). Esterification of dihydrocaffeic acid with polyunsaturated alcohols (linolenyl alcohol) and into polyunsaturated glycerides (linoleyl and linolenyl) results in rather poor antiradical activity (*49*, *50*). The present work demonstrated that association of the ferulate moiety with monounsaturated lipids (FDOG) leads to effective antiradical activity. Monounsaturated fatty acids are less prone to oxidation than their polyunsaturated counterparts, which may permit the feruloyl moiety an opportunity to quench radical species not present within itself. Moreover, FDOG retains its antioxidative capacity when incorporated into a bilayer (**Figure 2** and **Table 1**) and disperses evenly throughout the membrane plane, not forming domains. A positioning of the feruloyl moiety near the hydrophilic/hydrophobic interface (**Figure 7**) may promote greater activity toward a flux of radicals coming from the aqueous phase. Therefore, FDOG should be able to protect other entities present in the bilayer from free radical species.

FDOG incorporated into model phospholipid bilayers without an overt disruption of bilayer integrity (calcein—cobalt complex leakage test). This is clear because the leakage percentage (**Figure 3**) and leakage rates (**Table 2**) are virtually the same for all measurements. The lack of large variations in the leakage kinetics indicates that one single step was involved in the leakage mechanism (*51*). It is also interpreted that the shape of the leakage kinetics further indicates that the leakage mechanism was similar for all cases. Presumably, this means that FDOG does not induce any packing changes within the bilayer, as tighter packing is expected to lead to a lower leakage percentage (and possibly a slower rate) and looser packing is expected to lead to a greater leakage percentage (and rate). As for the location of FDOG within the bilayer, the feruoyl group proximity correlated well with the headgroup of DOPC lipids, suggesting that FDOG lipophilic behavior is similar to that of DOPC.

The FDOG extended conformation is similar to conformations studied in recent PM3 semiempirical calculations on cis-isomers of free unsaturated fatty acids, including oleic acid (*52*). However, the extended conformation of FDOG therefore permits its seamless insertion into the membrane. This finding is contrary to the stated expectation of Anselmi and co-workers (*38*) that a branched-chain, straight conformation, feruloyl ester would not fit well into a bilayer. This feature may be an asset that diminishes the potential of the molecule to express cytotoxic effects.

Any number of disease states and aging phenomena can be ascribed to a causal initiating influence of reactive oxygen and nitrogen species on cellular structures. Mitochondrial membranes are particularly susceptible to oxidative stressors. Lipophilic antioxidants such as FDOG could diminish membrane free radicals. Its mode of action would be similar to that of the natural lipophilic antioxidants vitamin E and lipoic acid. The results of this study demonstrated that FDOG incorporates into model membranes at significant levels without disrupting the membranes and displayed potent antioxidative capacity. Unlike simple alkyl esters of ferulic acid, the triacylglycerol structure of FDOG adopts an extended structure that places the feruloyl group close to the membrane aqueous/lipid interface. Furthermore, FDOG disperses throughout the membrane, which should afford greater protection to the membrane lipids and proteins.

ACKNOWLEDGMENT

We are indebted to Leslie Smith, Judy Blackburn, and Ray Holloway for their technical assistance.

Supporting Information Available: S1, HPLC chromatogram of purified FDOG; S2, electrospray ionization mass spectrometry (ESI-MS) analysis of FDOG; explanation of how NMR was used to distinguish 1(3)-feruloyl-2,3(1)-dioleoyl glycerol from 2-feruloyl-1,3-dioleoyl glycerol; S3, proton NMR of FDOG in spectral range for determining the position of ferulate substitution; S4, complete FDOG proton NMR spectrum in deuterated acetone; S5, FDOG HMBC spectrum; S6, ^{13}C assignments for FDOG; S7, NOESY spectrum of FDOG; S8, fluorescence spectra of FDOG; Table 1. Basis set dependence of relative energies for B3LYP geometry optimization calculations of conformations of ferulic acid. This material is available free of charge via the Internet at http://pubs.acs.org.

LITERATURE CITED

(1) Clifford, M. N. Chlorogenic acids and other cinnamates − nature, occurrence and dietary burden. *J. Sci. Food Agric*. **1999**, *79*, 362–372.
(2) Zhao, Z.; Moghadasian, M. H. Chemistry, natural sources, dietary intake and pharmacokinetic properties of ferulic acid: a review. *Food Chem*. **2008**, *109*, 691–702.
(3) Garça, J.; Pereira, H. Suberin structure in potato periderm: glycerol, long-chain monomers, and glyceryl and feruloyl dimers. *J. Agric. Food Chem*. **2000**, *48*, 5476–5483.
(4) Yunoki, K.; Musa, R.; Kinoshita, M.; Tazaki, H.; Oda, Y.; Ohnishi, M. Presence of higher alcohols as ferulates in potato pulp and its radical-scavenging activity. *Biosci. Biotechnol. Biochem*. **2004**, *68*, 2619–2622.
(5) Schmutz, A.; Jenny, T.; Ryser, U. A caffeoyl−fatty acid−glycerol ester from wax associated with green cotton fibre suberin. *Phytochemistry* **1994**, *36*, 1343–1346.
(6) Cooper, R.; Gottlieb, H. E.; Lavie, D. New phenolic diglycerides from *Aegilops ovata*. *Phytochemistry* **1978**, *17*, 1673–1675.
(7) Wang, T.; Hicks, K. B.; Moreau, R. Antioxidant activity of phytosterols, oryzanol, and other phytosterol conjugates. *J. Am. Oil Chem. Soc*. **2002**, *79*, 1201–1206.
(8) Ou, S.; Kwok, K.-C. Ferulic acid: pharmaceutical functions, preparation and applications in foods. *J. Sci. Food Agric*. **2004**, *84*, 1261–1269.
(9) Murakami, A.; Kadota, M.; Takahashi, D.; Taniguchi, H.; Nomura, E.; Hosoda, A.; Tsuno, T.; Maruta, Y.; Ohigashi, H.; Koshimizu, K. Suppressive effects of novel ferulic acid derivatives on cellular responses induced by phorbol ester, and by combined lipopolysaccharide and interferon-gamma. *Cancer Lett*. **2000**, *157*, 77–85.
(10) Murakami, A.; Nakamura, Y.; Koshimizu, K.; Takahashi, D.; Matsumoto, K.; Hagihara, K.; Taniguchi, H.; Nomura, E.; Hosoda, A.; Tsuno, T.; Murata, Y.; Won Kim, H.; Kawabata, K.; Ohigashi, H. FA15, a hydrophobic derivative of ferulic acid, suppresses inflammatory responses and skin tumor promotion: comparison with ferulic acid. *Cancer Lett*. **2002**, *180*, 121–129.
(11) Uwai, K.; Osanai, Y.; Imaizumi, T.; Kanno, S.; Takeshita, M.; Ishikawa, M. Inhibitory effect of the alkyl side chain of caffeic acid analogues on lipopolysaccharide-induced nitric oxide production in RAW264.7 macrophages. *Bioorg. Med. Chem*. **2008**, *16*, 7795–7803.
(12) Jayaprakasam, B.; Vanisree, M.; Zhang, Y.; Dewitt, D. L.; Nair, M. G. Impact of alkyl esters of caffeic and ferulic acids on tumor cell proliferation, cyclooxygenase enzyme, and lipid peroxidation. *J. Agric. Food Chem*. **2006**, *54*, 5375–5381.

(13) Fiuza, S. M.; Gomes, C.; Teixeira, L. J.; Girão da Cruz, M. T.; Cordeiro, M. N. D. S.; Milhazes, N.; Borges, F.; Marques, M. P. M. Phenolic acid derivatives with potential anticancer properties: a structure—activity relationship study. Part 1: Methyl, propyl and octyl esters of caffeic and gallic acids. *Bioorg. Med. Chem.* **2004**, *12*, 3581–3589.
(14) Comporti, M. Three models of free radical-induced cell injury. *Chem.-Biol. Interact.* **1989**, *72*, 1–56.
(15) Compton, D. L.; Laszlo, J. A.; Berhow, M. A. Lipase-catalyzed synthesis of ferulate esters. *J. Am. Oil Chem. Soc.* **2000**, *77*, 513–519.
(16) Laszlo, J. A.; Compton, D. L.; Eller, F. J.; Taylor, S. L.; Isbell, T. A. Packed-bed bioreactor synthesis of feruloylated monoacyl- and diacylglycerols: clean production of a "green" sunscreen. *Green Chem.* **2003**, *5*, 382–386.
(17) Choo, W.-S.; Birch, E. J. Radical scavenging activity of lipophilized products from lipase-catalyzed transesterification of triolein with cinnamic and ferulic acid. *Lipids* **2009**, *44*, 145–152.
(18) Compton, D. L.; Laszlo, J. A.; Berhow, M. A. Identification and quantification of feruloylated mono- and diacylglycerols from vegetable oils. *J. Am. Oil Chem. Soc.* **2006**, *83*, 753–758.
(19) MacDonald, R. C.; MacDonald, R. I.; Menco, B. P.; Takeshita, K.; Subbarao, N. K.; Hu, L. Small-volume extrusion apparatus for preparation of large, unilamellar vesicles. *Biochim. Biophys. Acta* **1991**, *1061*, 297–303.
(20) Evans, K. O. Room-temperature ionic liquid cations act as short-chain surfactants and disintegrate a phospholipid bilayer. *Colloids Surf., A* **2006**, *274*, 11–17.
(21) Zhang, J.; Stanley, R. A.; Melton, L. Lipid Peroxidation inhibition capacity assay for antioxidants based on liposomal membranes. *Mol. Nutr. Food Res.* **2006**, 714–724.
(22) Naguib, Y. M. A. A fluorometric method for measurement of peroxyl radical scavenging activities of lipophilic antioxidants. *Anal. Biochem.* **1998**, *265*, 290–298.
(23) Cao, G.; Alessio, H. M.; Cutler, R. G. Oxygen-radical absorbance capacity assay for antioxidants. *Free Radical Biol. Med.* **1993**, *14*, 303–311.
(24) Naguib, Y. M. A. Antioxidant activities of astazanthin and related carotenoids. *J. Agric. Food Chem.* **2000**, *48*, 1150–1154.
(25) Davenport, L.; Dale, R. E.; Bisby, R. H.; Cundall, R. B. Transverse location of the fluorescent probe 1,6-diphenyl-1,3,5-hexatriene in model lipid bilayer membrane systems by resonance excitation energy transfer. *Biochemistry* **1985**, *24*, 4097–4108.
(26) Wolf, D. E.; Winiski, A. P.; Ting, A. E.; Bocian, K. M.; Pagano, R. E. Determination of the transbilayer distribution of fluorescent lipid analogues by nonradiative fluorescence resonance energy transfer. *Biochemistry* **1992**, *31*, 2865–2873.
(27) Mukherjee, S.; Raghuraman, H.; Dasgupta, S.; Chattopadhyay, A. Organization and dynamics of N-(7-nitrobenz-2-oxa-1,3-diazol-4-yl)-labeled lipids: a fluorescence approach. *Chem. Phys. Lipids.* **2004**, *127*, 91–101.
(28) Kachel, K.; Asuncion-Punzalan, E.; London, E. The location of fluorescence probes with charged groups in model membranes. *Biochim. Biophys. Acta* **1998**, *1374*, 63–76.
(29) Kondo, M.; Mehiri, M.; Regen, S. L. Viewing membrane-bound molecular umbrellas by parallax analyses. *J. Am. Chem. Soc.* **2008**, *130*, 13771–13777.
(30) Lewis, B. A.; Engelman, D. M. Lipid bilayer thickness varies linearly with acyl chain length in fluid phosphatidylcholine vesicles. *J. Mol. Biol.* **1983**, *166*, 211–217.
(31) Anselmi, C.; Centini, M.; Granata, P.; Sega, A.; Buonocore, A.; Bernini, A.; Facino, R. M. Antioxidant activity of ferulic acid alkyl esters in a heterophasic system: a mechanistic insight. *J. Agric. Food Chem.* **2004**, *52*, 6425–6432.
(32) Klamt, A.; Schüürmann, G. COSMO: A new approach to dielectric screening in solvents with explicit expressions for the screening energy and its gradient. *J. Chem. Soc., Perkin Trans.* **1993**, *2*, 799.
(33) Shimanouchi, T.; Ishii, H.; Yoshimoto, N.; Umakoshi, H.; Kuboi, R. Calcein permeation across phosphatidylcholine bilayer membrane: effects of membrane fluidity, liposome size, and immobilization. *Colloids Surf., B* **2009**, *73*, 156–160.
(34) Evans, K. O.; Lentz, B. R. Kinetics of lipid rearrangements during poly(ethylene glycol)-mediated fusion of highly curved unilamellar vesicles. *Biochemistry* **2002**, *41*, 1241–1249.
(35) Peng, X.; Chen, H.; Draney, D. R.; Volcheck, W.; Schutz-Geschwender, A.; Olive, D. M. A nonfluorescent, broad-range quencher dye for Förster resonance energy transfer assays. *Anal. Biochem.* **2009**, *388*, 220–228.
(36) Morris, J. V.; Mahaney, M. A.; Huber, J. R. Fluorescence quantum yield determinations. 9,10-Diphenylanthracene as a reference standard in different solvents. *J. Phys. Chem.* **1976**, *80*, 969–974.
(37) Fattal, D. R.; Ben-Shaul, A. Mean-field calculations of chain packing and conformational statistics in lipid bilayers: comparison with experiments and molecular dynamics studies. *Biophys. J.* **1994**, *67*, 963–995.
(38) Anselmi, C.; Centini, M.; Andreassi, M.; Buonocore, A.; La Rosa, C.; Maffei Facino, R.; Sega, A.; Tsumo, F. Conformational analysis: a tool for the elucidation of the antioxidant properties of ferulic acid derivatives in membrane models. *J. Pharm. Biomed. Anal.* **2004**, *35*, 1241–1249.
(39) Bakalbassis, E. G. A density functional theory study of structure-activity relationships in caffeic and dihydrocaffeic acids and related monophenols. *J. Am. Oil Chem. Soc.* **2003**, *80*, 459–466.
(40) Sebastian, S.; Sundaraganesan, N.; Manoharan, S. Molecular structure, spectroscopic studies and first-order molecular hyperpolarizabilities of ferulic acid by density functional study. *Spectrochim. Acta, Part A* **2009**, *74*, 312–323.
(41) Calheiros, R.; Borges, F.; Marques, M. P. M. Conformational behaviour of biologically active ferulic acid derivatives. *J. Mol. Struct. THEOCHEM* **2009**, *913*, 146–156.
(42) Machado, N. F. L.; Caheiros, R.; Gaspar, A.; Garrido, J.; Broges, F.; Margques, M. P. M. Antioxidant phenolic esters with potential anticancer activity: solution equilibria studied by Raman spectroscopy. *J. Raman Spectrosc.* **2009**, *40*, 80–85.
(43) Calheiros, R.; Machado, N. F. L.; Fiuza, S. M.; Gaspar, A.; Garrido, J.; Milhazes, N.; Borges, F.; Marques, M. P. M. Antioxidant phenolic esters with potential anticancer activity: A Raman spectroscopy study. *J. Raman Spectrosc.* **2008**, *39*, 95–107.
(44) Ge, M.; Zhao, H.; Wang, W.; Zhang, Z.; Yu, X.; Li, W. Terahertz time-domain spectroscopy of four hydroxycinnamic acid derivatives. *J. Biol. Phys.* **2006**, *32*, 403–412.
(45) Silva, F. A. M.; Borges, F.; Guimarães, C.; Lima, J. L. F. C.; Matos, C.; Reis, S. Phenolic acids and derivatives: studies on the relationship among structure, radical scavenging activity, and physicochemical parameters. *J. Agric. Food Chem.* **2000**, *48*, 2122–2126.
(46) Nenadis, N.; Zhang, H.-Y.; Tsimidou, M. Z. Structure−antioxidant activity relationship of ferulic acid derivatives: effect of carbon side chain characteristic groups. *J. Agric. Food Chem.* **2003**, *51*, 1874–1879.
(47) Fang, X.; Shima, M.; Kadota, M.; Tsuno, T.; Adachi, S. Suppressive effect of alkyl ferulate on the oxidation of linoleic acid. *Biosci. Biotechnol. Biochem.* **2006**, *70*, 457–461.
(48) Kikuzaki, H.; Hisamoto, M.; Hirose, K.; Akiyama, K.; Taniguchi, H. J. Antioxidant properties of ferulic acid and its related compounds. *J. Agric. Food Chem.* **2002**, *50*, 2161–2168.
(49) Sabally, K.; Karboune, S.; Yeboah, F. K.; Kermasha, S. Lipase-catalyzed esterification of selected phenolic acids with linolenyl alcohols in organic solvent media. *Appl. Biochem. Biotechnol.* **2005**, *127*, 17–27.
(50) Sabally, K.; Karboune, S.; Kermasha, S. Lipase-catalyzed transesterification of triolein or trilinolenin with selected phenolic acids. *J. Am. Oil Chem. Soc.* **2006**, *83*, 101–107.
(51) Thorén, Per E.G.; Söderman, O.; Engström, S.; von Corswant, C. Interactions of novel, nonhemolytic surfactants with phospholipid vesicles. *Langmuir* **2007**, *23*, 6956–6965.
(52) Vysotsky, Y. B.; Belyaeva, E. A.; Fainerman, V. B.; Vollhardt, D.; Aksenenko, E. V.; Miller, R. Thermodynamics of the clusterization process of *cis* isomers of unsaturated fatty acids at the air/water interface. *J. Phys. Chem. B* **2009**, *113*, 4347–4359.

Received for review January 29, 2010. Revised manuscript received April 1, 2010. Accepted April 3, 2010. Names are necessary to report factually on available data; however, the USDA neither guarantees nor warrants the standard of the product, and the use of the name by the USDA implies no approval of the product to the exclusion of others that may also be suitable.